J. Austral. Math. Soc. 19 (Series B), (1975), 229–241.

CONTACT PROBLEM OF AN ELASTIC PLUG IN AN ELASTIC REGION

G. P. STEVEN

(Received 4 September 1975)

Abstract

The contact problem investigated in this paper may be more fully described as a three dimensional elastic body with a circular hole through it; inside this tunnel is press fitted a solid elastic plug of finite length. Shear stresses are taken to be absent along the contact interface.

An influence coefficient technique is used to model the governing integral equation. For the elastic region the displacement influence coefficients due to bands of constant pressure are determined using a numerical quadrature on Fourier integrals. However, the plug, being of finite length, requires the superposition of two separate solutions to boundary value problems before the displacement influence coefficients can be determined.

Contact pressure distributions are presented for a sample of parameter variations and also for a case where hydrostatic pressure is present in the tunnel in the elastic region. Despite both components being elastic the imposition of a constant interference displacement along the interface still gives rise to the characteristic singularity in contact pressure at the edges of contact due to the strain discontinuity at these points.

1. Introduction

In this paper the contact between an elastic finite length solid cylinder press fitted inside a cylindrical tunnel through an infinite elastic region is studied. The elastic-elastic problem is the true representation of the behaviour of two bodies in contact. The Hertzian solution for two curved surfaces is one of the few closed form solutions available for such elastic-elastic contact. Most work in the past, (see Galin [8] for a review of plane contact problems), has concentrated on the case where one of the bodies involved is rigid.

For the axisymmetric shrink-fit type situation a few elastic-elastic solutions exist. Some consider thin shell collars shrunk-fit onto elastic shafts [5], [6], [22]. The thick collar case was presented by Okubo [18] wherein some approximations had to be made to simulate stress free boundary conditions on axial sections at the ends of the collar. However, solutions to shrink-fit problems of the nature presented herein have received little attention.

The technique of the solution develops as the work proceeds and it need not be mentioned at this stage.

2. The contact problem and governing field equations

The region with the circular hole can be regarded as being sufficiently large in the axial and radial directions for the stresses set up by the interference fit to have decayed almost to zero. In the radial direction the decay is as one over radius squared and in the axial direction St. Venant's principle applies since the stress distribution set up by the contact is self equilibrating and at several times the contact radius away axially from this there would be little effect. These arguments serve to indicate where infinity lies for the region. It is also assumed that slip between the two contacting components has taken place, thus the shear stress is zero along the contact interface. Under these conditions the governing integral equation for a contact length of L, can be expressed as,

$$u(z) = \int_{-L/2}^{L/2} \{u_r(z, z') - u_c(z, z')\} p(z') dz', \tag{1}$$

where $u(z)$ is the prescribed interference fit along interface,

$u_{r,c}(z, z')$ radial displacement of region/cylinder at z due to unit ring loading of pressure at z',

$p(z')$ loading function, defined only within interface, all other surface tractions being zero.

This integral equation can be solved by representing it as a finite series of linear algebraic equations as follows,

$$u[n] = \sum_{m=1}^{2N} \{u_r[n, m] - u_c[n, m]\} p[m]. \tag{2}$$

The kernel or Green's function in the original integral equation now has a different significance. Whereas $u(z, z')$ in (1) is defined in terms of a unit ring of pressure, $u[n, m]$ is now the mean radial displacement in the nth finite length segment of the contact region (there being $2N$ equal segments to the total contact length L), due to a band of unit pressure in the mth segment. This implies that the contact pressure distribution is no longer continuous but step-wise continuous. It is a simple task to solve such equations and even more so if the interference displacement is symmetrical about the centre of the plug as the number of linear equations is now N in N unknown values of pressure. This influence coefficient technique has been shown to give good results even for a small number of segments [4], [5], [24]. For the results presented herein a value of $N = 10$ is used throughout. It now remains to present details as to how the displacement influence coefficients $u_r[n, m]$ and $u_c[n, m]$ are derived for both components of the shrink-fit assembly.

The basic field equations for stress and displacement which are required can be extracted from the Papkovich-Neuber solutions to the displacement form of the axisymmetric equilibrium equations [24], [19], [17], [7], and [14].

$$\begin{aligned} u = [&C_1\{4(1-\nu)I_1(\beta x) - x\beta I_0(\beta x)\} \\ &+ C_2\{4(1-\nu)K_1(\beta x) + \beta x K_0(\beta x)\} \\ &+ C_3\{-\beta I_1(\beta x)\} + C_4\{\beta K_1(\beta x)\}]\cos\beta\zeta, \end{aligned} \tag{3}$$

$$\begin{aligned} w = [&C_1\{x\beta I_1(\beta x)\} + C_2\{x\beta K_1(\beta x)\} + C_3\{\beta I_0(\beta x)\} \\ &+ C_4\{\beta K_0(\beta x)\}]\sin\beta\zeta, \end{aligned} \tag{4}$$

$$\begin{aligned} \frac{r_0}{2G}\sigma_{rr} = \Big\{ &C_1\left[(3-2\nu)\beta I_0(\beta x) - \left\{\frac{4(1-\nu)}{x} + \beta^2 x\right\} I_1(\beta x)\right] \\ &+ C_2\left[-(3-2\nu)\beta K_0(\beta x) - \left\{\frac{4(1-\nu)}{x} + \beta^2 x\right\} K_1(\beta x)\right] \\ &+ C_3\left[\frac{\beta}{x} I_1(\beta x) - \beta^2 I_0(\beta x)\right] \\ &+ C_4\left[-\frac{\beta}{x} K_1(\beta x) - \beta^2 K_0(\beta x)\right]\Big\}\cos\beta\zeta, \end{aligned} \tag{5}$$

$$\begin{aligned} \frac{r_0}{2G}\sigma_{\theta\theta} = \Big\{ &C_1\left[\frac{4(1-\nu)}{x} I_1(\beta x) - (1-2\nu)\beta I_0(\beta x)\right] \\ &+ C_2\left[\frac{4(1-\nu)}{x} K_1(\beta x) + (1-2\nu)\beta K_0(\beta x)\right] \\ &+ C_3\left[-\frac{\beta}{x} I_1(\beta x)\right] + C_4\left[\frac{\beta}{x} K_1(\beta x)\right]\Big\}\cos\beta\zeta, \end{aligned} \tag{6}$$

$$\frac{r_0}{2G}\sigma_{zz} = \{C_1[2\nu\beta I_0(\beta x) + \beta^2 x I_1(\beta x)]$$
$$+ C_2[-2\nu\beta K_0(\beta x) + \beta^2 x K_1(\beta x)] \tag{7}$$
$$+ C_3[\beta^2 I_0(\beta x)] + C_4[\beta^2 K_0(\beta x)]\}\cos\beta\zeta,$$

$$\frac{r_0}{2G}\sigma_{rz} = \{C_1[\beta x I_0(\beta x) - 2(1-\nu)I_1(\beta x)]$$
$$+ C_2[-\beta x K_0(\beta x) - 2(1-\nu)K_1(\beta x)] + C_3[\beta I_1(\beta x)] \tag{8}$$
$$+ C_4[-\beta K_1(\beta x)]\}\,\beta\sin\beta\zeta,$$

where $x = r/r_0$, $\zeta = z/r_0$, (r, z) are cylindrical coordinates
r_0 is some non-dimensionalising radius,
ν is Poisson's ratio,
β is an arbitrary parameter,
C_1 to C_4 are constants of integration.
Equations (3) to (8) may now be used as a basis for the evaluation of the required displacement influence coefficients.

3. Influence coefficients for circular hole in elastic region

Only two references are available for this class of boundary value problem, the first by Westergaard [30] uses a very approximate method and it is difficult to make any assessment of his results. However the other by Tranter [27] using a Fourier transform method and evaluating the resulting Fourier integrals by quadrature, provided a useful basis for comparison with results obtained in the process of solving the problem herein.

In the general field equations for stress and displacement applied to this type of region the I type Bessel functions need be ignored due to their singularity at infinity. Applying the boundary conditions $\sigma_{rr} = -p_0\cos\beta\zeta$, $\sigma_{rz} = 0$ on $x = 1$ yields the following expression for the radial displacement on $x = 1$.

$$u_{r,x=1} = \frac{p_0 r_0}{2G}\left[\frac{2(1-\nu)K_1^2(\beta)}{\beta\chi(\beta)}\right]\cos\beta\zeta$$
$$\chi(\beta) = \beta^2[K_1^2(\beta) - K_0^2(\beta)] + 2(1-\nu)K_1^2(\beta). \tag{9}$$

For the desired boundary condition of a band of constant pressure of length "$2b$" the following boundary conditions prevail.

$$\sigma_{rr} = -p(\zeta), \qquad \sigma_{rz} = 0 \text{ on } x = 1 \tag{10}$$

where

$$p(\zeta) = \begin{cases} p_0 & \text{for} \quad \zeta < b \\ 0 & \text{for} \quad \zeta > b. \end{cases}$$

The function $p(\zeta)$ can be represented by the Fourier integral,

$$p(\zeta) = \int_0^\infty p(\beta) \cos \beta\zeta d\beta,$$

where $p(\beta)$, the Fourier transform is given by,

$$p(\beta) = \frac{2}{\pi} \int_0^\infty p(\zeta) \cos \beta\zeta d\zeta = 2p_0 \sin \beta b / \pi\beta,$$

thus,

$$p(\zeta) = \frac{2p_0}{\pi} \int_0^\infty \frac{\sin \beta b \cos \beta\zeta}{\beta} d\beta.$$

Applying the Fourier integral to the radial displacement gives the following expression for the radial displacement at any point along the surface $x = 1$.

$$u_r = \frac{p_0 r_0}{\pi G} \int_0^\infty \left[\frac{2(1-\nu)K_1^2(\beta)}{\beta \chi(\beta)} \right] \sin \beta b \cos \beta\zeta d\beta. \tag{11}$$

The nature of the K type Bessel functions rules out the possibility of evaluating the desired displacement by the contour integration technique of Lur'e [15]. This is because the presence of a logarithmic term in the series expansion for K makes them multivalued. Thus there is no need to determine the roots of the equation $\chi(\beta) = 0$. This conclusion was reached by a different course by Steven [25], where it is indicated that $\chi(\beta)$ has in fact no distinct roots but is zero along a continuous line in the complex β plane, rendering the use of contour integration impossible.

Thus a direct quadrature technique is used to determine the displacement for a series of values of b and at values of ζ corresponding to the mid point of the segments into which the contact length is divided.

The limiting value of the integrand in (11) as $\beta = 0$ is $b/2(1-\nu)$ and the computer using rational polynomial approximations to the Bessel functions was able to generate this value to an accuracy of 10^{-7}. At high values of β (> 200 say) the asymptotic expressions for the K's are used and it can be shown that the integrand's asymptotic form is $(\sin \beta b \cos \beta\zeta)/\beta^2$ which can be decomposed to a combination of sine terms and cosine integrals. Some sample calculations of the radial displacement were made in order to compare values with those of Tranter [27] who used a similar technique but incorporated the truncated asymptotic expansions for $\beta > 12$. For $b = 0.5$, $\zeta = 0$ the difference in values was within 0.1%. Another check was made with $b = 10$ which gave a value at $\zeta = 0$ of 0.9972 of the Lamé solutions for plane stress solution. With these various checks carried out it was then possible to compute a series of the displacement influence coefficients for a series of values of b. These may then be matched to any set of coefficients for the finite length plug provided the contact length is the same.

4. Influence coefficients for finite length solid cylinder

In order to determine the desired influence coefficients a technique has been devised which separates the boundary value problem into two separate boundary value problems. Firstly the cylinder is considered to be infinite in length and by a similar technique to that used for the region with a hole influence coefficients can be calculated by direct quadrature from the equation,

$$u_c = -\frac{p_0 r_0}{\pi G}\int_0^\infty \left[\frac{2(1-\nu)I_1^2(\beta)}{\beta\phi(\beta)}\right]\sin\beta b\cos\beta\zeta\, d\beta,$$
$$\phi(\beta) = \beta^2[I_0^2(\beta) - I_1^2(\beta)] - 2(1-\nu)I_1^2(\beta). \tag{12}$$

At the same time as the displacements are being evaluated, the stresses σ_{zz} and σ_{rz} can be calculated using the expressions

$$\sigma_{zz} = -\frac{2p_0}{\pi}\int_0^\infty \left[\frac{2\beta I_1(\beta)I_0(\beta x) + \beta^2 x I_1(\beta)I_1(\beta) - \beta^2 I_0(\beta)I_0(\beta x)}{\beta\phi(\beta)}\right] \times \sin\beta b\cos\beta\zeta\, d\beta, \tag{13}$$

$$\sigma_{rz} = -\frac{2p_0}{\pi}\int_0^\infty \left[\frac{\beta x I_1(\beta)I_0(\beta x) - \beta I_0(\beta)I_1(\beta x)}{\phi(\beta)}\right]\sin\beta b\sin\beta\zeta\, d\beta. \tag{14}$$

These stresses are evaluated at a series of values of x and at values of ζ corresponding to the desired locations of the end faces of the finite length cylinder. Since the lack-of-fit is taken to be symmetrical, then by superposition the end face stresses due to two unit pressure bands symmetrically disposed can be obtained, these will give a self equilibrating stress system.

The second boundary value problem now arises in that, having established the stress distribution on surfaces corresponding to the location of the ends of the finite length cylinder, these surfaces have to be made stress free by applying equal and opposite stress distributions. This is now what is called the end load problem with no tractions on the radial surfaces of the cylinder and thus the homogeneous solution to the governing field equations is required.

Many references are available for non-homogeneous boundary value

https://doi.org/10.1017/S0334270000001107 Published online by Cambridge University Press

problems for solid circular cylinders. For the homogeneous or end load case several works are available, see for instance, Horvay and Mirabal [10], Mendelson and Roberts [16], Kaehler [11], Warren and Roark [28], Blair and Veeder [2], Hodgkins [9], Warren, Roark and Bickford [29], Little and Childs [13], Widera and Wu [31], Swan [26], Shibahara and Oda [23], Chandrashekhara [3], Klemm and Little [12], Power and Childs [20], Benthem and Minderhoud [1].

The technique adopted herein is similar to that of Little and Childs [13] whereby the end stresses σ_{zz} and σ_{rz} are expressed in terms of a series of eigen functions associated with the eigen values produced by the homogeneous boundary conditions on the radial surfaces. The eigen values are in fact extracted from the equation $\phi(\beta) = 0$, see equation (12), and are tabulated in many references cf. [24], [15], [11], [28] and [13]. The series for the radial displacements axial stress and shear stress are as follows.

$$u = \sum_s \left\{ \frac{D_s}{I_1(\beta_s)} \left[-xI_0(\beta_s x) + \left[\frac{2(1-\nu)}{\beta_s} + \frac{I_0(\beta_s)}{I_1(\beta_s)} \right] I_1(\beta_s x) \right] e^{i\beta_s\zeta} \right\} \tag{15}$$

$$\frac{r_0\sigma_{zz}}{2G} = \sum_s \left\{ \frac{D_s}{I_1(\beta_s)} \left[\left(2 - \beta_s \frac{I_0(\beta_s)}{I_1(\beta_s)} \right) I_0(\beta_s x) + x\beta_s I_1(\beta_s x) \right] e^{i\beta_s\zeta} \right\} \tag{16}$$

$$\frac{r_0\sigma_{rz}}{2G} = \sum \left\{ \frac{-iD_s}{I_1(\beta_s)} \left[\beta_s x I_0(\beta_s x) - \beta_s \frac{I_0(\beta_s)}{I_1(\beta_s)} I_1(\beta x) \right] e^{i\beta_s\zeta} \right\} \tag{17}$$

Using a least squares technique the coefficients D_s can be evaluated from the stress boundary conditions on the ends of the finite length cylinder. Thus the radial displacement may be evaluated using equation (15) and together with that from the pressure band solution on the infinite length cylinder make up the desired influence coefficients for this part of the contact assembly.

5. Numerical results

The two lots of displacement influence coefficients can be brought together and assembled into equation (2) for solution. Due to the many parameters involved only a sample selection of the results are presented. However for all cases investigated the same general characteristics, which are observed from the results given herein, are present. In order to make the pressure and displacement values non-dimensional the Lamé plane stress solution is used, this is those values which would have resulted had the contact region been infinite in length. These are expressed as follows where G is the shear modulus, ν Poisson's ratio, the subscripts r, c and ls denote the region, cylinder and Lamé solution respectively, the contact radius is unity, and δ is the lack-of-fit, ($\delta = u[n]$ in equation (2)),

$$p_{ls} = 2\delta G_r G_c(1+\nu_c)/[G_c(1+\nu_c)+G_r(1-\nu_c)],$$

$$u_{c,ls} = p_{ls}\,(1-\nu_c)/2G_c\,(1+\nu_c), \qquad u_{r,ls} = p_{ls}/2G_r.$$

Figure 1 shows the variation of p/p_{ls} against ζ/L with $\nu_c = \nu_r = 0.3$, $G_c = G_r$ and L varying between 0.4 and 8. These curves all illustrate the common characteristic of an edge singularity. This is to be expected since the use of a constant lack-of-fit along the interface gives rise to a discontinuity in strain at the edge of the region and consequently the stress singularity. Such singularities are absent only when there is zero interference at the edge of the region.

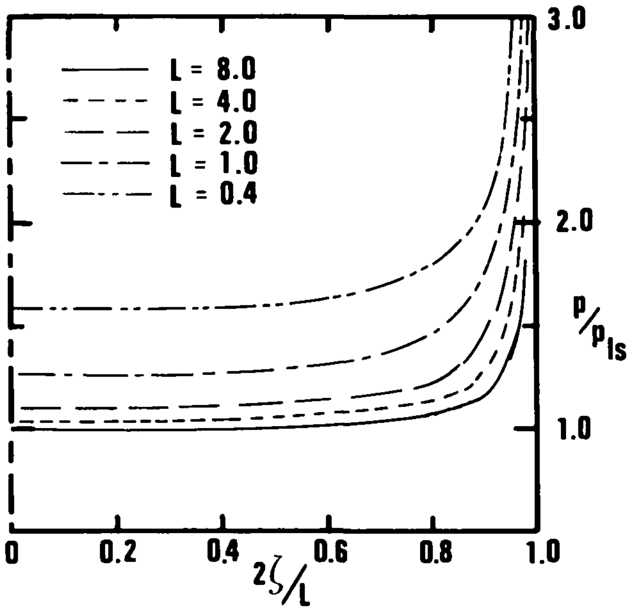

Figure 1. p/p_{ls}, finite length solid cylinder shrunk-fit into elastic region, for $\nu_c = \nu_r = 0.3$, $G_c = G_r$ and various L.

For large contact lengths the contact pressure is very close to the Lamé solution for most of the contact region. At the other limit for small L the values of pressure are significantly different from the Lamé solution, indeed with such a short length the effect of the axisymmetric terms in the governing differential equations is reduced and in the limit as $L \to 0$ is removed. This situation is more appropriate to the plane strain indentation of a half space and it has been shown in other work, Steven [24], that in the case of shrink-fit problems with collars on shafts, with $L = 0.02$, the pressure distribution is almost identical to such a half space indentation solution given by Sadowsky [21] as $p = P/\pi(a^2 - \zeta^2)^{1/2}$ where P is the total load, a is the 1/2 width of indentation and p is the contact pressure.

Figure 2 has the same data as Figure 1 except that ν_c is now 0.5 and it is observed that little difference exists between the pressure distributions with the change in Poisson's ratio of the cylinder. This is a general characteristic of contact problems that Poisson's ratio has little or no effect on interference pressure distributions.

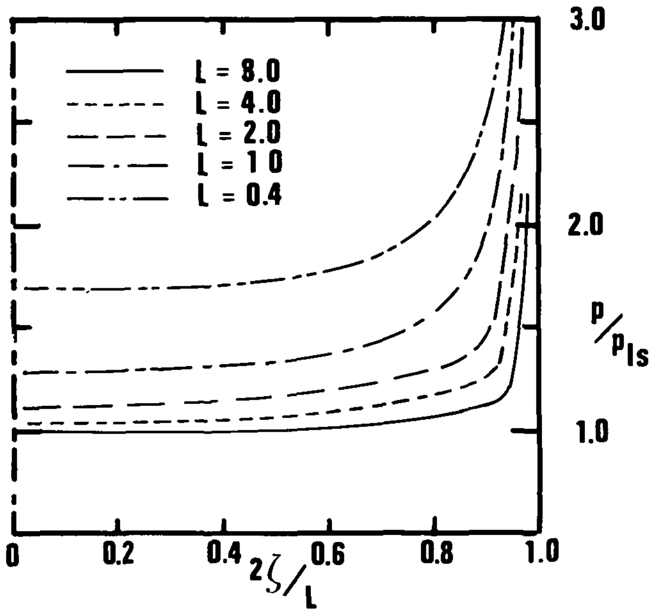

Figure 2. p/p_{ls}, finite length solid cylinder shrunk-fit into elastic region, for $\nu_c = 0.5$, $\nu_r = 0.3$, $G_c = G_r$ and various L.

In Figure 3 the displacement distribution along the contact interface is plotted for various values of the modular ratio G_r/G_c showing how the proportions of the lack-of-fit are taken up as this ratio varies. The situation where a greater proportion is taken up by one component as its modulus

https://doi.org/10.1017/S0334270000001107 Published online by Cambridge University Press

reduces in relation to that of the other component is to be expected. The common aspect of all the curves is the increase of the u_c/δ values at the edge of the region; this is due simply to the reduction in stiffness at the ends of the cylinder whereas the region continues on beyond this point thus supplying a greater reinforcement to the region.

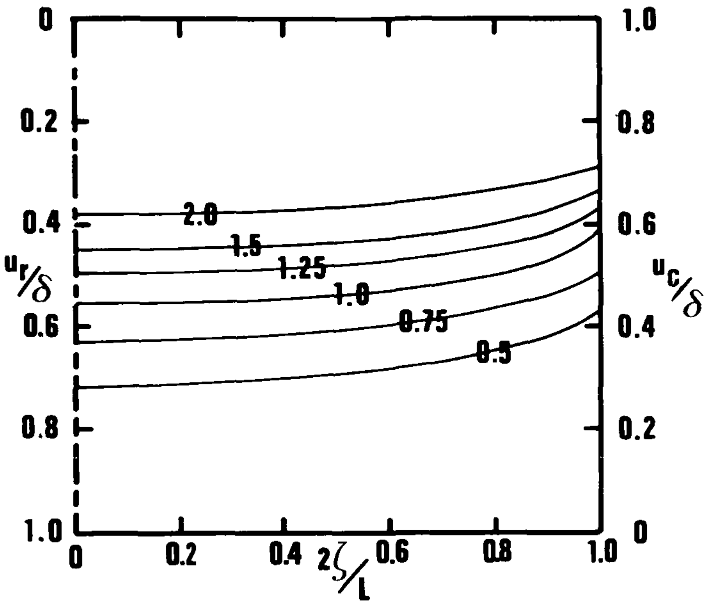

Figure 3. u_c/δ and u_r/δ, finite length solid cylinder shrunk-fit into elastic region, for $\nu_c = \nu_r = 0.3$, $L = 1.0$ and various modular ratio G_r/G_c.

An interesting extension of the work previously detailed is to apply a hydrostatic pressure f on all surfaces except the contact interface, see Figure 4. Its effect on the cylindrical plug is to give a Poisson's ratio radial expansion of $\nu_c f/2G_c(1+\nu_c)$, for a unit non-dimensionalised radius. On the region the effect of the hydrostatic pressure can be obtained using an extension of the work detailed in Section 3 of this paper. By considering bands of constant normal pressure, where the bandwidth is very large (i.e. > 10) on either side of the plug, the resulting radial displacement due to unit hydrostatic pressure ($f = 1$) at the mid-point of each segment along the contact interface can be calculated. The amended form of the simultaneous linear equations (2), to allow for these effects, is,

$$u[n]+f\left[\frac{\nu_c}{2G_c(1+\nu_c)}-u_{r'f}[n]\right]=\sum_{m=1}^{N}P_m\{u_r[n,m]+u_c[n,m]\}\qquad(19)$$

where $u_{r'f}[n]$ is the radial displacement in the nth segment due to unit hydrostatic pressure on either side of the contact region.

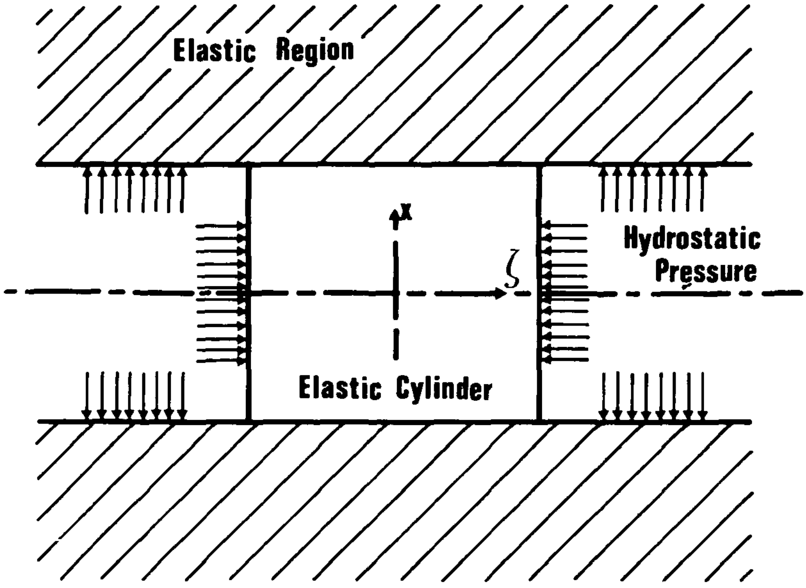

Figure 4. Finite length solid cylinder shrunk-fit into infinite elastic region with hydrostatic pressure acting.

In Figure 5 plots of p/p_{ls} with $\nu_r = \nu_c = 0.3$, $G_r = G_c$, $L = 1$ and various values of $h = f/p_{ls}$ are presented. From this it is seen that with increasing h the pressure in the edge portion of the contact region increases while in the centre portion it decreases. To explain this it is necessary to consider the left hand side of equation (19) wherein it can be said that the term $u_{r'f}[n]$ is small at the edge of the contact region and larger in the centre. This means that the lack-of-fit is greater at the edge and smaller in the centre and with increasing h the difference between these two increases, thus the contact pressure will follow these trends. Eventually the reduction of lack-of-fit at the centre of the region is such that the lack-of-fit becomes zero, that is the surfaces separate and this is indicated by the zero pressure portion at $h = 15.38$.

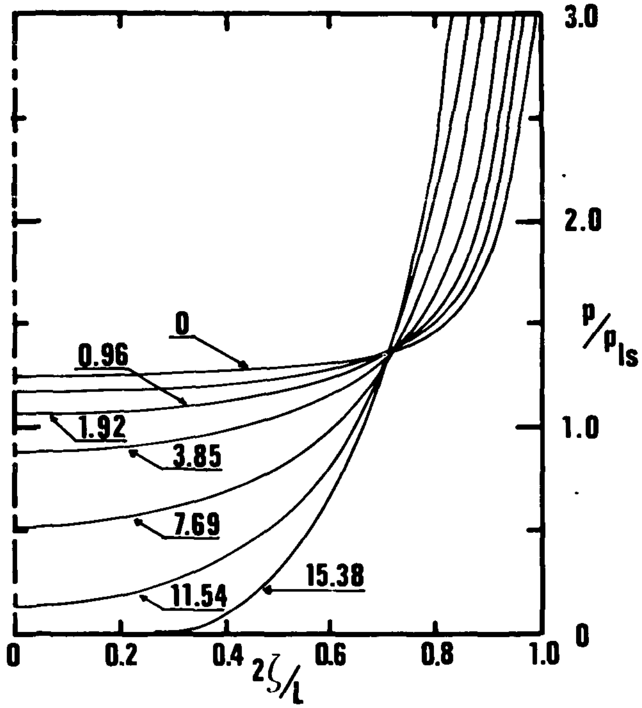

Figure 5. p/p_{ls}, hydrostatic pressure effect on finite length solid cylinder shrunk-fit into elastic region, for $\nu_c = \nu_r = 0.3$, $G_r = G_c$, $L = 1.0$ and various h.

6. Conclusion

The solution of contact problems by the displacement influence coefficient technique has been shown to be a method of great generality in so much as having calculated influence coefficients for one set of parameters for either body in contact, these can be matched to any other set for the other body provided the contact lengths are the same. This avoids the necessity of solving the whole problem each time for every set of parameters. Also it enables the total boundary value problem to be considered as a series of separate simpler boundary value problems especially the case of the finite length cylinder.

Results obtained herein all conform to the classical pattern for rigid indentation, however by considering both components to be elastic more appropriate practical conclusions may be taken from such results. Clearly the singularities present in all cases presented in this paper are easily removed by ensuring that the relative displacement between the two bodies is zero at the edge of the contact region.

Further work in this area could consist of the inclusion of non slipped or

https://doi.org/10.1017/S0334270000001107 Published online by Cambridge University Press

partially slipped cases, more appropriate stress-strain relationships in the high stress regions and non symmetric or non uniform lack-of-fit distributions.

Acknowledgements

The author wishes to acknowledge the editor and staff of this Journal for their assistance in the preparation of this paper.

References

[1] J. P. Benthem and P. Minderhoud, *Int. J. Solids. Struct.* 8 (1972) 1027.
[2] J. M. Blair and J. I. Veeder, *J. of Appl. Mech.* 36 (1969) 241.
[3] K. Chandrashekhara, *AIAA J.* 7 (1969) 1161.
[4] H. D. Conway and K. A. Farnham, *Int. J. of Engng. Sci.* 5 (1967) 541.
[5] H. D. Conway and K. A. Farnham, *Int. J. of Mech. Sci.* 10 (1968) 757.
[6] R. A. Eubanks, *Proc. 8th Midwest. Mech. Conf.* 2 (1963) 84.
[7] M. B. Galerkin, *Comptes Rendus. Acad. Sci.*, Paris 190 (1930) 1047.
[8] L. A. Galin, *Contact Problems in the Theory of Elasticity*, North Carolina State College (1961).
[9] W. R. Hodgkins, *UKAEA TRG Rpt.* 294 (1962).
[10] G. Horvay and J. A. Mirabal, *J. Appl. Mech.* 25 (1958) 561.
[11] H. Kaehler, *AIAA J.* 3 (1965) 2132.
[12] J. L. Klemm and R. W. Little, *SIAM J. Appl. Maths.* 19 (1970) 712.
[13] R. W. Little and S. B. Childs, *Q. Appl. Math.* 25 (1967) 261.
[14] A. E. H. Love, *A Treatise on the Mathematical Theory of Elasticity*, Dover, (1944).
[15] A. I. Lur'e, Three Dimensional Problems in the Theory of Elasticity, *Interscience* (1964).
[16] A. Mendelson and E. Roberts, *Midwest. Tech. Conf. Case. Inst. Tech.* (1963).
[17] H. Neuber, *Z. Angew. Math. Mech.* 14 (1934).
[18] H. Okubo, *Z. Angew. Math. Mech.* 12 (1952) 178.
[19] P. F. Papkovich, *Izvest. Akad. Nauk.* SSSR, 10 (1932) also *Comptes Rendus. Acad. Sci.*, Paris, 192 (1932) 513.
[20] L. D Powers and S. B. Childs, *Int. J. Engng. Sci.* 9 (1970) 241.
[21] M. A. Sadowsky, *Trans. ASME*, paper no. APM–54–21 (1932) 221.
[22] R. T. Severn, *Q. J. Mech. Appl. Math.* 12 (1952) 178.
[23] M. Shibahara and J. Oda, *Bull. JSME* 11 (1968) 1000.
[24] G. P. Steven, D. Phil Thesis, The University of Oxford (1970).
[25] G. P. Steven, *Int. J. of Engng. Sci.* 11 (1973) 795.
[26] G. W. Swan, *SIAM J. Appl. Math.* 16 (1968) 860.
[27] C. J. Tranter, *Quart. J. of Appl. Maths.* 4 (1964) 298.
[28] W. E. Warren and A. L. Roark, *AIAA J.* 5 (1967) 1484.
[29] W. E. Warren, A. L. Roark and W. B. Bickford, *AIAA J.* 5 (1967) 1448.
[30] H. M. Westergaard, Karman Anniversary Volume, (1941) 154.
[31] O. E. Widera and C. H. Wu, *J. Engng. Maths.* 2 (1968) 343.

Department of Aeronautical Engineering,
The University of Sydney,
Sydney, N.S.W., 2006,
Australia.